Spring 5-2013

Studies on Controlling the Morphology of an Organic Bulk-Heterojunction Photovoltaic Device to Improve its Efficiency

Kelly R. McLeod
University of Southern Mississippi

The University of Southern Mississippi

Studies on Controlling the Morphology of an Organic Bulk-Heterojunction Photovoltaic Device to Improve its Efficiency

By

Kelly McLeod

A Thesis
Submitted to the Honors College of
The University of Southern Mississippi
in Partial Fulfillment
of the Requirements for the Degree of
Bachelor of Science
in the Department of Polymers and High Performance Materials

April 2013

Approved by

_____

Sarah E. Morgan
Professor of Polymer Science

_____

Robert Y. Lochhead, Director
School of Polymers and High
Performance Materials

_____

David R. Davies, Dean
Honors College

ABSTRACT

A systematic study of the effects of alteration of processing parameters in combination with incorporation of polyhedral oligomeric silsesquioxane (POSS) molecules on the properties and structure of bulk heterojunction organic photovoltaic cells made from P3HT:PCBM blends was undertaken. On implementing the correct processing protocol, incorporation of POSS molecules with specific structures resulted in considerable enhancement in cell efficiencies. Octaaminophenyl POSS incorporation resulted in a 20% increase in cell efficiency over the control and caused the formation of crystalline, fiber-like structures in the active layer of the photovoltaic cell.

TABLE OF CONTENTS

LIST OF FIGURES AND TABLES

LIST OF ABBREVIATIONS

AFM	Atomic force microscopy
D/A	Donor/acceptor
HOMO	Highest occupied molecular orbital
ITO	Indium tin oxide
LUMO	Lowest unoccupied molecular orbital
nm	Nanometer
OAP	Octaaminophenyl
OPV	Organic photovoltaic cell
PAP	Phenylaminopropyl
PCBM	[6,6]-Phenyl-C_{61}-buyric acid methyl ester
PEDOT:PSS	Poly(3,4-ethylenedioxythiophene):poly(styrenesulfonate)
P3HT	Poly(3-hexylthiophene)
POSS	Polyhedral oligomeric silsesquioxane
UV-Vis	Ultraviolet-visible

ACKNOWLEDGEMENTS

I would like to acknowledge and thank my research advisor, Dr. Sarah Morgan, for her guidance and support the past two years. Her advice will no doubt guide me well as I advance in my career, and her patience with me is more than I deserve. I would also like to acknowledge the role that Dr. Mithun Bhattacharya played in expanding my knowledge of photovoltaics and thank him for his patience in teaching me how to make photovoltaic cells. His mentorship was invaluable and he generously performed atomic force microscopy on my samples and assisted in the analysis of the results. I would also like to thank the rest of the Morgan Research Group for their support and aid, especially Qi Wu.

I would like to thank my parents, Bruce and Christine McLeod, and siblings, Alex and Sheila, for their unwavering support and encouragement in all my endeavors. I would like to thank the rest of my family both for the pride they have in me and for the personal motivation they inspire.

Funding from The U.S. Department of Energy under grant number DE-EE0003173 and from the Ray C. Anderson Foundation is gratefully acknowledged. I would also like to thank Hybrid Plastics, Inc. for donation of the POSS materials and for useful discussions.

CHAPTER I

INTRODUCTION

1.1 Introduction

In the past thirty years, the demand for more environmentally friendly and reliable sources of energy has funded research into photovoltaics, better known as solar cells. These photovoltaic cells can convert the ultimate renewable resource—light—into electricity. Currently, there are already inorganic based photovoltaic cells that have efficiencies as high as 40%.[1] Such inorganic solar cells are already available commercially in the form of solar panels. Most inorganic cells are made of a special grade of silicon that must undergo extensive processing before the solar cell can be made. The cost of this processing—both in terms of energy needed to accomplish the processes and the financial cost—means that inorganic cells have to function for years before performance can offset the production and maintenance costs. [2] However, in recent years research interest has been shifted to studying organic photovoltaics (OPV).

Organic photovoltaic cells start with many advantages over inorganic cells. OPV cells are made of thin films (100 nm) coated onto a substrate. The substrate needs only to be transparent and stable to the conditions the cell would encounter—meaning that normal plastic sheets could be used, rather than specially grown silicon wafers. Not only would the substrate be cheaper, the very nature of the *thin* film means that the amount of material needed to make a cell would be minimal. The processing of such a cell would also be cheap and easy because the chemicals could be printed or spin coated onto the substrate. Also, the number and nature of the organic materials that could be used for photovoltaics allows for cells to be "tuned" for different properties. Despite all of the

advantages of OPV, current research has not been able to produce a cell with a high enough efficiency to compete with the inorganics. The best bulk heterojunction cells made have had efficiencies of over 5%, but theoretical calculations indicate that efficiencies of $\underset{\sim}{}$10% are possible and would be economically competitive.[2] Research in photovoltaics is working on reaching that benchmark.

1.2 Organic Photovoltaic

Before the details of photovoltaic research can be discussed, a basic understanding of the workings of an OPV device must be established. A device generally is comprised of multiple layers: the transparent substrate (glass, plastic), a transparent conducting oxide (the anode), a hole transporting layer, the active layer, an electron transporting layer, and a metal layer (cathode). A cross section of such a cell can be seen in Figure 1.2.1. The substrate is an inert material that provides physical support for the other layers. The anode is the entrance for current to flow into the cell, while the cathode is the exit for current. The active layer is made of a combination of an electron donor and an electron acceptor. Figure 1.2.2 contains visual representation of the process undergone once the photons from sunlight enter the OPV device and cause the formation of an exciton in the donor. An exciton is what forms when an electron is excited (such as by photons) in an organic semiconductor; the electron moves to a higher energy state.[3]

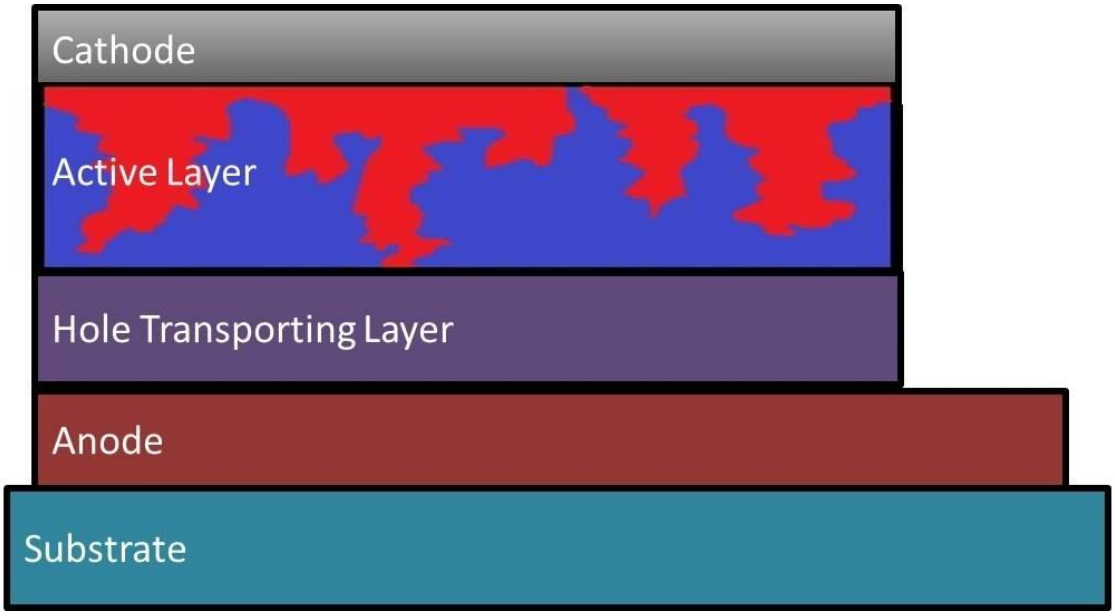

Figure 1.2.1. Cross Section of Bulk Heterojunction Photovoltaic Cell

Once the excitons are formed, they start to diffuse throughout the donor. If the interface between the donor and acceptor is encountered, charge separation can occur, but there needs to be an existing electric field to unbind the exciton into free charges. The electric field is caused by the different work functions of the electrodes. Once the electron is unbound from its hole, the electric field transports it to the cathode while the hole travels to the anode. The hole is the slightly positively charged area left behind in the electron's original energy state. The anode and cathode collect the charges and drive them into an electric circuit.[4].This process is not always perfect; if the interface between the donor and acceptor polymers is too great a distance from the site of exciton formation, the exciton will decay. There can also be charge recombination where the hole and the electron recombine after being separated.[3] The last layer, the hole transport layer, is a layer between the active layer and the anode that prevents the flow of electrons to the

anode and only allows holes to pass through. Some cells have an additional electron transporting layer between the cathode and the active layer.

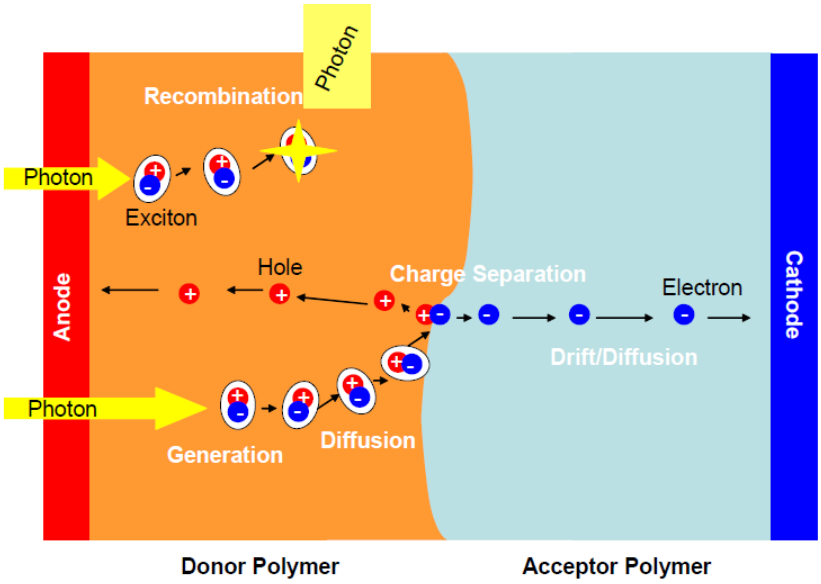

Figure 1.2.2. Schematic of Mechanism of Charge Production and Transport in Photovoltaic Cell. Copied from Figure 6, page 14 of Salamamdra.[5]

1.3 *Characteristics*

Discussing cell performance also requires knowledge of the characteristics of a working cell. The basic current-voltage curve is shown in Figure 1.3.1. The short circuit current (I_{sc}) is the current in the cell when there is no applied voltage; the open circuit voltage (V_{oc}) is the voltage when there is no current. The largest rectangle that fits under the current/voltage curve is the maximum experimental power, P_{max}, or I_{max} multiplied by V_{max}. There is another rectangle formed by I_{sc} multiplied by V_{oc}, which corresponds to the maximum theoretical power of the device. The fill factor (FF) is a dimensionless number that is equivalent to the maximum experimental power divided by the maximum theoretical power of the device.

$$FF = \frac{P_{max}}{I_{sc} \times V_{oc}}$$

Another characteristic commonly discussed is the efficiency of an OPV device. The efficiency, η, is the percentage of the power actually generated by the cell to the amount of power impinged upon the device by the light. This impinging power is found by multiplying the energy of illumination (G) by the surface area of the cell (S).

$$\eta = \frac{P_{max}}{G \times S}$$

This is how the previously mentioned efficiencies of photovoltaic cells were calculated.[7]

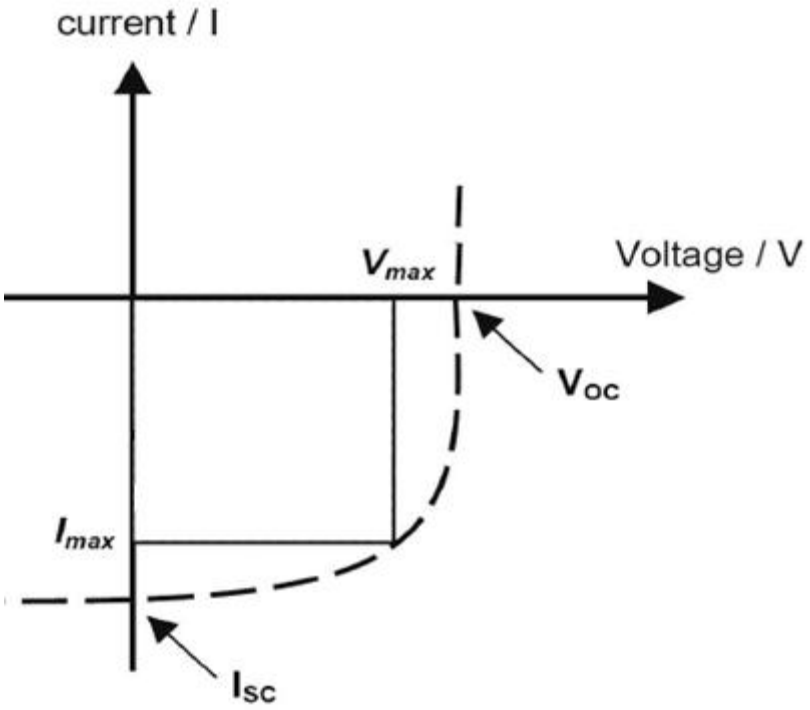

Figure 1.3.1. Example Current-Voltage Characteristic Curve

Understanding the basic functions and characteristics of an OPV cell allows the more complex characteristics to be described. There are two major factors that limit the

efficiency of an OPV cell. The first has to do with the band gap of a donor/acceptor (D/A) pair. Band gap is the difference between the highest occupied molecular orbital (HOMO) of the donor and lowest unoccupied molecular orbital (LUMO) of the acceptor. The band gap is relatively fixed for a set of polymers and the only way to easily alter the gap is to change the polymer pair. Band gap is important because it determines the wavelengths of light that a pair can harvest. The current problem is that most of the existing D/A pairs have a band gap of around 2 eV, which absorbs light near 600 nm.[8] The maximum photon flux of the sun, where the greatest number of photons are produced, is around 700 nm. Band gaps smaller than 2 eV are required to get maximum absorption near that value. While it is important to realize that the band gap plays a large role in the efficiency of photovoltaics, it is a quality that is not easily manipulated.[4] The best way to change the band gap is to change to a completely different D/A pair. The other and the more tailorable efficiency limiting factor is the morphology of the D/A pair. The morphology controls how well the excitons and subsequently the free electrons and holes move through the active layer, not only in how far the quasiparticles have to move but also in ease of movement. The goal of morphology control is to get all excitons to the D/A interface and then get all resulting charges to the respective electrodes. The degree of crystallinity in the active layer, the extent of phase separation, and the solubility and self-assembly of the polymers themselves are all factors that affect the morphology of the system in a complex relationship that determines the efficiency. These factors can be manipulated and studied until the optimum combination is found. Previously, thermal and solvent vapor annealing has been used to manipulate the morphology, but the underlying science is not well understood.[12] The goal of my research is to incorporate nanoparticles

into the active layer to directly change the morphology. We hypothesize that the presence of the nanoparticles will force the ordering of the D/A phases, leading to enhanced absorption and charge carrier mobility, and hence, improved efficiency.

1.4 *Bulk Heterojunction*

There are three main types of organic photovoltaic cell active layer architectures: a single layer, or Schottky; a bilayer heterojunction; and a bulk heterojunction. In a single layer cell, there is not a donor/acceptor pair but one organic layer and the two electrodes. In a bilayer heterojunction, the donor and the acceptor are each in separate layers, one on top of the other. In a bulk heterojunction device, the donor and acceptor are mixed together in one cell but phase separated.[9] A bulk heterojunction cell helps prevent charge recombination while still maintaining a smaller path distance to the donor/ acceptor interface. In a single layer system, holes and electrons move through the same medium and this greatly enhances the chance of recombination. In a double layer system, the holes and electrons are separated but the interface may be too far from the site of exciton formation and the exciton decays before reaching it. In a bulk heterojunction, the donor and acceptor polymers are separate but interpenetrating, allowing a larger interface but enough separation to reduce recombination.[6] However, the bulk heterojunction's efficiency relies heavily on morphology. The pair must be mixed thoroughly to achieve the correct interpenetration but the separate domains must also be large enough to allow movement to the interface and to the electrodes without much interference. The ideal morphology would look something like weaving the teeth of two combs together. This would represent a large interface (where the teeth touch) while still maintaining the

continuous pathways needed for effective transport. Unfortunately, the real morphology more closely resembles two types of bubbles mixed together to form random domains of donor and acceptor.

1.5 Annealing

Thermal annealing has been found to increase the overall efficiency of a device. It increases the degree of crystallinity in P3HT, which at once decreases the separation between chains and increases the interchain interactions. The effect of this is increased hole mobility in P3HT. However, thermal annealing also increases the phase separation of the active layer, increasing individual domain sizes. Figure 1.5.1 illustrates this effect. The larger domain size decreases the number of pathways in the PCBM network, which leads to a decrease in electron mobility in PCBM.[10] It has also been shown to decrease the efficiency of exciton quenching at the interface of the D/A pair. This happens, again, because of the increase of phase separation—there is a greater distance between the donor and the acceptor and so the exciton transfer is not as efficient.[11] Also, if the domains become too crystalline the edges of the crystal grains can create resistance and decrease the current the device produces.

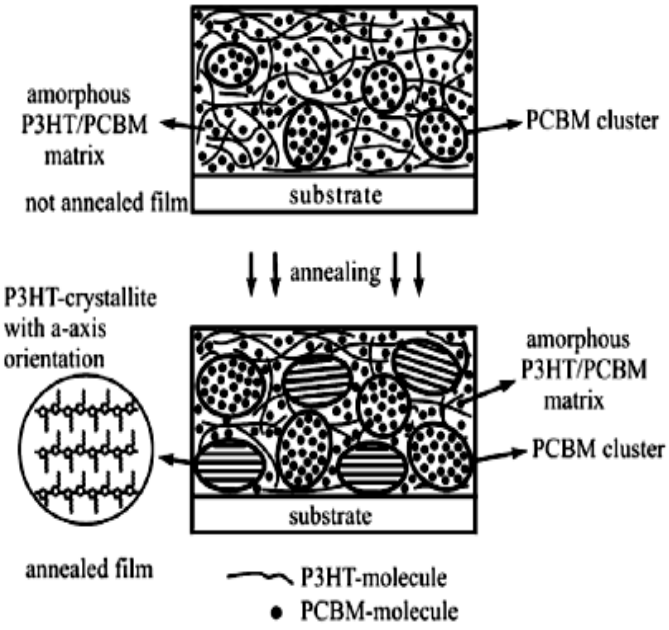

Figure 1.5.1. Effect of Annealing on Morphology Figure copies from Figure 3, page 1326 of Dennler et al..[2]

The overall increase in the efficiency of the cell can be attributed to the fact that while P3HT starts out with poor hole mobility, PCBM starts with good electron mobility. So the increase in the hole mobility helps more than the decrease in electron mobility hurts. However, a morphological study performed by Jo et al.[12] gave insight into how to gain the benefits of thermal annealing without the negatives. When the active layer is thermally annealed, PCBM forms clusters and aggregates and prevents P3HT from forming large crystalline structures. If solvent vapor annealing, or allowing the active layer to slowly dry in a chamber containing saturated solvent vapor, is used rather than thermal annealing, the P3HT forms long fibrillar structures while the PCBM aggregates more slowly. The higher crystallinity of the P3HT raises its HOMO level, which in turn lowers the band gap, improving efficiency. It is hypothesized that a judicious choice of solvent is necessary to enable the concurrent self-assembly of the donor phase and the

mobility of the acceptor fullerenes. This could ensure sufficient intermixing of the blend while avoiding chances of large scale phase separation of the D/A phases. Both thermal and solvent vapor annealing had individual benefits, but combining the two methods can result in a cell that is even more efficient. Performing solvent vapor annealing to promote P3HT crystallization followed by thermal annealing to allow PCBM aggregation (while maintaining the P3HT structure) can provide the benefits of both annealing processes.

1.6. *Materials*

The devices made for this study will use already well-established materials. The transparent anode will be made of indium tin oxide (ITO). A glass substrate will be used. These will be paired with an aluminum cathode. The donor polymer that will be used is poly(3-hexylthiophene) (P3HT). The acceptor molecule is the fullerene derivative [6,6]-phenyl-C_{61}-butyric methyl ester (PCBM). The donor and acceptor pair structures are shown in Figure 3.2.1. To the left is the highly conjugated polymer used as the donor,P3HT. The fullerene derivative to the right is the acceptor, PCBM.[6] A hole transporting layer is used between the anode layer (ITO) and active layer (P3HT and PCBM); this layer will be composed of the polymer mixture of poly(3,4-ethylenedioxythiophene) (PEDOT) and poly(styrenesulfonate) (PSS). This hole transporting layer facilitates the efficient transfer of the hole to the anode after charge disassociation. Using this combination of materials has several advantages. The main advantage is that the focus of the study can be narrowed considerably, because many parameters and procedures are already well understood and can be implemented without change. In this study, the only parameters to be changed will be the processing conditions

used to produce the active layer. The effects of changes in processing parameters on device performance will thus be directly measured. Another advantage of well-established materials is that they are readily commercially available. Other researchers have manufactured air processed cells using a similar system to that used in this study; these devices have reported efficiencies in the 2-4% range[17-20].

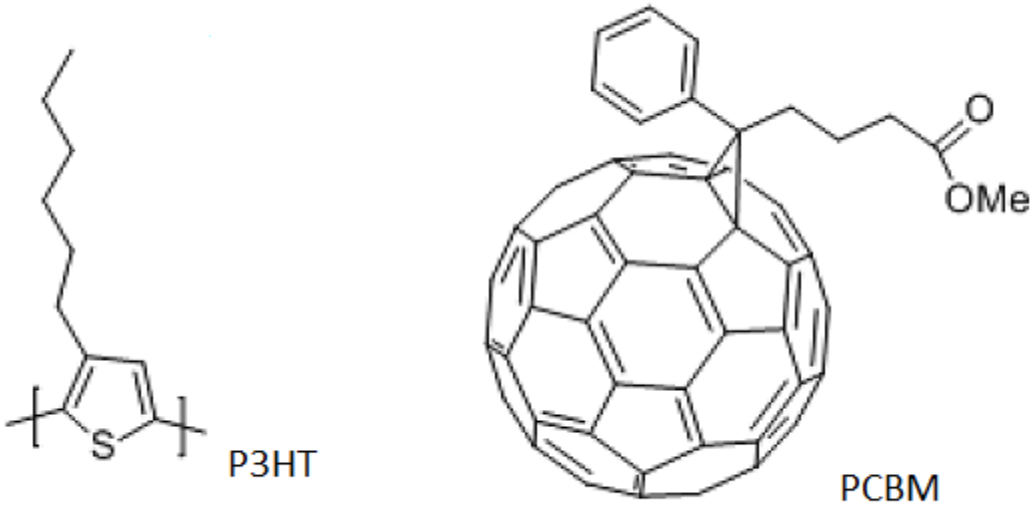

Figure 1.6.1. Structures of Donor (P3HT) and Acceptor (PCBM).

1.7 *Polyhedral Oligomeric Silsesquioxane*

In this study, we intend to use polyhedral oligomeric silsesquioxane (POSS) to alter the morphology of the active layer. POSS is a hybrid organic-inorganic molecular that consists of an inorganic cage structure with organic moieties attached. The general structure of a POSS molecule can be seen in Figure 1.6.1. Previous research in our laboratories indicated that POSS can change the surface morphology of nylon-6,[13] and Paul et al. observed phase separation in thin films of poly (tert-butyl acrylate)/POSS

blends.[14] However, no other research has used POSS as a morphology modifier in an OPV system. Based on the thin film examples, it is expected that the presence of POSS will have some discernible effect on the morphology. It is hypothesized that POSS molecules with tailored functionalities will preferably interact with one of the D/A phases and force them to order around it and create an overall more favorable morphology.

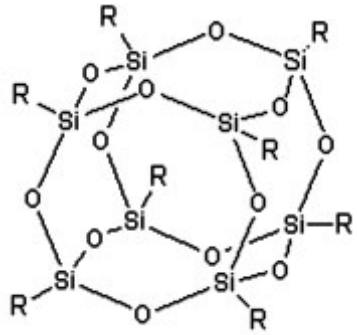

Figure 1.7.1. POSS Inorganic Cage Structure.

CHAPTER II

GOALS AND OBJECTIVES

This study will design and study methods to improve the efficiency of an organic bulk heterojunction photovoltaic device by controlling the morphology. The goals of the study are as follows: A) to find the optimal processing conditions for thermal annealing and solvent vapor annealing and B) to incorporate polyhedral oligomeric silsesquioxane into the active layer as a morphology modifier. In optimizing the processing, it is hypothesized that careful solvent choice for solvent vapor annealing will enable both the ordering of the donor phase and an increase in the mobility of the acceptor phase and that there is some combination of solvent vapor annealing and thermal annealing that maximizes the efficiency of the cell. The hypothesis for the second part of the study is that POSS with certain functionalities will, upon incorporation in the active layer, interact with the D/A phases and force ordering that ultimately creates a more favorable morphology.

CHAPTER III

EXPERIMENTAL METHODS

3.1 Introduction

This is a two-part study; in first part of the study, device manufacturing and annealing processes were varied to determine the factors affecting solar cell performance. A standard, reproducible processing method was defined. In the second part of the study, the effects of incorporation of nanomaterials on the morphology of the active layer and on solar cell efficiency were determined, in an attempt to establish structure-property relationships. A cell efficiency tester coupled to a solar simulator was used to determine the efficiency, while the morphology was probed using atomic force microscopy (AFM), x-ray diffraction spectroscopy (XRD), and ultraviolet-visible absorption spectroscopy (UV-Vis). All current-voltage curves are representative of an average of six cells, while the other characterization techniques were performed at least twice.

The cell efficiency tester generates the current-voltage characteristic curve discussed in the introduction. AFM is a method that uses a probe to tap the surface of active layer. AFM studies allow generation of nano-scale topological images, mapping of the current in conductive films, and relative modulus of phase separated domains. XRD uses x-rays to generate spectral peaks, whose size and spacing correlate with the overall crystallinity of a system. The information from these peaks can be used with the Scherrer equation to find the crystallite domain size. Information generated using UV-Vis indicates the amount of light absorbed by the system as well as the optical band gap, crystallinity and π-π stacking in the system. Combining, these techniques will help

illuminate the correlation between morphology changes and efficiency, and thus establish structure-property relationships in these OPV cells.

3.2 *Materials*

Of the materials used to makes the photovoltaic cell, the encapsulation epoxy and the PEDOT:PSS mixture were purchased from Ossila Ltd. The ITO printed glass slides were provided by Luminescence Technology Corp. The solvents used as well as the P3HT and PCBM were purchased from Sigma Aldrich. All components purchased from Sigma Aldrich were of purity 99% or greater. The P3HT used was regioregular electronic grade with number average molecular weight between 54,000-75,000 g/mol.

Two different types of POSS, donated by Hybrid Plastics Inc., were also used in the active layer of the cells. One was a straight-chain primary amine called octaaminophenyl POSS (OAP) with an aromatic ring, while the other was a slightly branched secondary amine, also with an aromatic ring. The second is referred to as phenylaminopropyl POSS (PAP).

3.3 *Active Layer Solution Preparation*

The active layer was prepared in a standard approach. It was made in 2 mL batches, where 19.0 mg of PCBM and 31.6 mg of P3HT were weighed and added to an amber vial with 2 mL dichlorobenzene, to achieve a P3HT/PCBM weight ratio of 1:0.6. This vial was set as-is into an oil bath at 60 °C for one hour. The oil bath was then turned off and both the bath and vial were left for twenty-four hours to facilitate controlled P3HT crystal precursor generation in the solution stage. Once this time had passed, the

active layer was then ready to be used. For the POSS samples, 1% of POSS by weight of solids was added after the twenty-four hours and the solution was sonicated in a Fisher Scientific FS20D sonicator for 15 minutes.

3.4 *Preparation of Organic Photovoltaic Cell*

The organic photovoltaic cells were made in batches of three. First, the ITO-coated glass substrates were cleaned by ultrasonication in three solvents: deionized water, acetone, and then isopropanol. The cleaned substrates were then placed in an ultraviolet and ozone cleaner for forty minutes. The process oxidizes the surface and promotes the adhesion of the hole transporting layer. The hole transporting layer was spin coated onto the ITO-coated substrate by dropping 50 μL of PEDOT:PSS onto the substrate at 5000 RPM and allowing the cell to spin for 120 s. The glass was then moved onto a hotplate at 150 °C for 10 minutes. Then 40 μL of the active layer was spin coated onto the substrate at 1250 RPM for 60 s using a Laurell Technologies Corp. WS-400B-GNDP/LITE spin coater. The cell was then placed in the solvent vapor annealing chamber for a certain time, as determined by the experiments to optimize annealing. The solvent used for the solvent vapor annealing was also determined during the optimization of annealing. Once the appropriate amount of time had passed, the cell was moved to the sputter coater. Once the sputter coater was vacuum sealed and under argon, the aluminum cathode was sputtered onto the cell using a Quorum Q150TES at a rate of 35 to 40 nm/min until 100 nm was deposited onto the cell. The cell was moved into a vacuum oven at 150 °C. The oven was purged with argon and left for a certain time, as determined by the experiments to optimize annealing. A drop of encapsulation epoxy was placed onto a cell to seal a

plain glass cover slip over the aluminum (this protects the cathode from oxidation, which would lower the efficiency). To cure the epoxy, the cell was exposed to UV-light for 6 minutes. Once the epoxy was cured, aluminum legs were pushed onto the edges of the cell in order to place the finished cell into the cell efficiency tester.

3.5 *Annealing Optimization*

The method used to find the optimal conditions was to vary each parameter, one at a time, and the optimum is the time or solvent that produces the most efficient cell. The four solvents used for solvent vapor annealing were o-dichlorobenzene, chlorobenzene, chloroform, and isopropanol. The solvent vapor annealing and thermal annealing times were varied between zero and sixty minutes at regular intervals. Each parameter was varied separately; the solvent vapor annealing time used to find the best solvent had earlier been optimized at 20 minutes.

3.6 *Cell Efficiency Test*

Current-voltage (J-V) measurements were carried out using a Keithley 2400 source unit. Irradiation was provided by an AM1.5 solar simulator (Photo Emission Tech. Inc, CA) with illumination of 1000 W/m2 from a Xenon lamp coupled to a monochromator. The total incident light intensity was calibrated with a standard reference silicon solar cell.

3.7 *X-Ray Diffraction Spectroscopy*

X-ray diffraction studies of the photovoltaic samples spin coated on unpatterened ITO glass subtrates were obtained using a Rigaku D/MAX-Ultima-III Diffractometer at room temperature using Cu Kα radiation at a tube current of 44 mA and an acceleration voltage of 40 kV. Scan range was 4° - 30° at a step interval of 0.01° and a scanning rate of 0.5°/min. The Scherrer Equation below was used to calculate the crystallite size of the sample.

$$\tau = \frac{K * \lambda}{\beta * \cos(\theta)}$$

For the equation, K is a shape factor, typically 0.9. The wavelength of the x-ray is λ, while β is the full-width at half-maximum of a baseline corrected peak. The θ corresponds to the Bragg angle. In addition to the crystallite size, the d-spacing of the crystal layers was calculated using Bragg's Law, seen below. The new variable introduced into this equation is d, which represents the d-spacing.

$$\lambda = 2 * d * \sin(\theta)$$

3.8 *Ultraviolet-Visible Absorption*

UV-vis spectra were obtained using a Perkin-Elmer Lambda 6 UV/Vis spectrophotometer. The spectral range in which data was obtained was 300 to 700 nm and spectra were normalized at 666 nm.

3.9 *Atomic Force Microscopy*

Atomic force microscopy studies on the samples were conducted on a Dimension ICON scanning probe microscope from Bruker (Santa Barbara, CA). A silicon probe with

a 115 μm long silicon nitride cantilever from Bruker, nominal force constant within 0.3 N/m, and resonance frequency of 47 kHz was used for surface topography studies in Scanasyst mode. AFM imaging was conducted under ambient conditions in a temperature (22 °C) and humidity (40-45%) controlled room.

CHAPTER IV

SAFTEY CONSIDERATIONS

Safety and environmental considerations have been taken into account for this research. The material safety data sheets have been consulted for all of the materials used for the purpose of this project. The most hazardous material is the active layer solution itself; it will be handled in a hood and disposed of in a properly labeled halogenated waste container. One should also avoid breathing the powdered materials, which are the PCBM, P3HT, OAP-POSS, and PAP-POSS. These become components of the active layer, whose safety considerations have already been discussed. The solvents used for solvent vapor annealing will be handled in a well-ventilated hood, with gloves, and the waste disposed in a properly labeled container.

CHAPTER V

SUMMARY OF EXPECTED RESULTS

It is expected that there is a combination of thermal annealing time, solvent used for vapor annealing, and solvent vapor annealing time that maximizes the efficiency of a photovoltaic cell. There should also be a discernible change in morphology upon incorporation of POSS into the active layer. OAP POSS has a straight chain primary amine possessing a rich π-electron cloud in the form of a phenyl ring. It is thus expected to facilitate more efficient packing, which would increase crystallinity and in-plane π–π stacking of the P3HT. Increasing crystallinity increases conjugation length, which ultimately increases the overall efficiency of the cell. The non-linear, secondary amine with a non-planar phenyl ring based POSS, PAP, is expected to have some effect on the morphology of the active layer but not facilitate greater crystallinity. It is the purpose of this research to probe the morphology changes seen by annealing processes and/or POSS presence and correlate these structural changes with the performance properties of the photovoltaic cell.

CHAPTER VI

RESULTS AND DISCUSSION

6.1 *Optimizing Device Manufacture and Annealing*

Current-voltage curves were used to optimize processing conditions by finding the conditions with highest efficiencies. The optimal conditions were a solvent vapor anneal of twenty minutes under isopropanol and thermal annealing of thirty minutes. Figure 6.1.1. displays the current-voltage curves for the different solvents used for solvent vapor annealing. Not only does the isopropanol curve have the highest efficiency, the use of it also results in the cell with the highest fill factor. The other three solvents used in the test can all be used to make the active layer; however, isopropanol was chosen because its solubility parameters fall between those of the donor and acceptor phase. Solvent vapor annealing with isopropanol allowed the P3HT to start self-assembly while allowing the PCBM to remain mobile. PCBM aggregation occurs during the thermal annealing stage.[12]

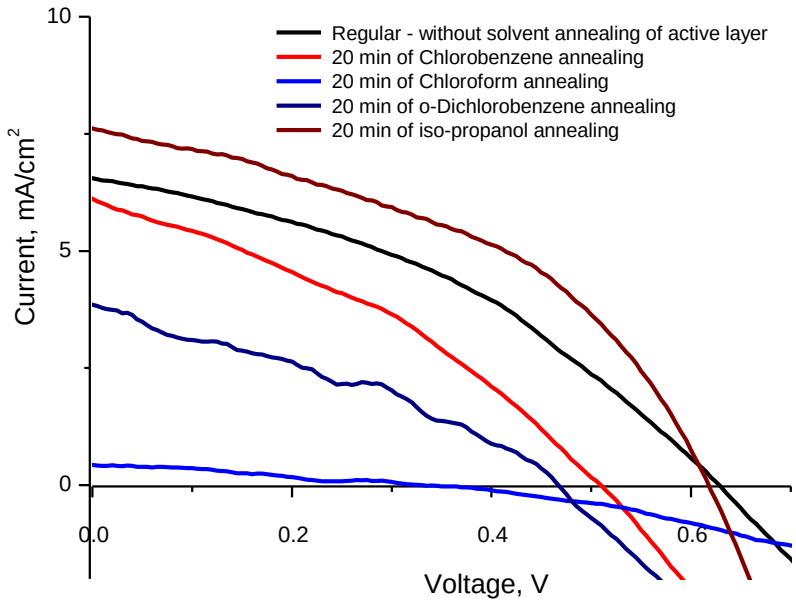

Figure 6.1.1 Current-Voltage Curves with Different Solvents

The time for each annealing stage was determined by varying the annealing time over an hour. The time that corresponded to the highest efficiency curve was chosen as the standard annealing time for future experiments. The combination of those three specific conditions more than doubled the efficiency. Figure 6.1.2. shows current-voltage curves at different thermal annealing times. The optimal annealing times were 20 minutes of solvent vapor annealing with isopropanol and 30 minutes of thermal annealing.

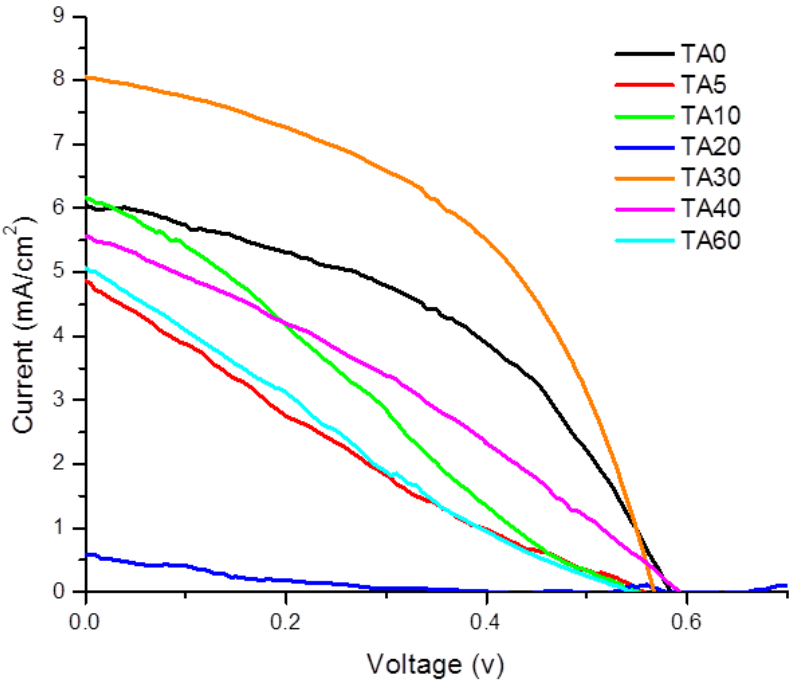

ıes

6.2 *Efficiency trends*

The effect of the addition of two different types of POSS on the efficiency of an organic photovoltaic cell was studied. These trends will then be used to examine the relationship between the morphology changes induces by the incorporation of POSS and the changes in efficiency. Figure 6.2.1 is a current-voltage curve for the average efficiency results. While OAP POSS increased the efficiency over that of the control, the PAP POSS significantly decreased the overall efficiency.

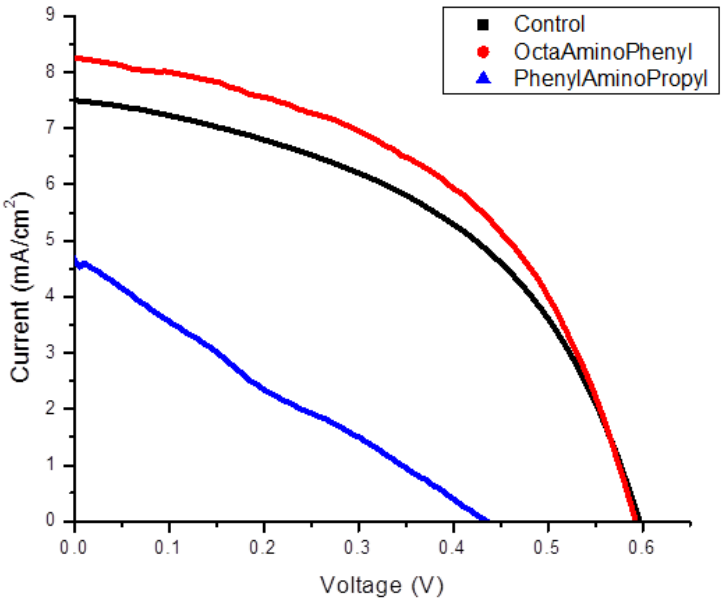

Figure 6.2.1 Current-Voltage Curve of POSS Modified Active Layers

The increase in the efficiency exhibited by the OAP POSS is a result of the increased fill factor and higher short circuit current, though the open circuit voltage remained relatively the same. The higher short circuit current is an indication of greater charge mobility in the system, while open circuit voltage depends more on the donor-acceptor pair and was not expected to change.[12] The maximum efficiencies for each active layer, both thermally and solvent vapor annealed, are as follows: for the control, 2.36%; for OAP POSS active layer, 2.79%; and for PAP POSS 0.63%. The OAP POSS containing active layer exhibited a power conversion efficiency about 20% higher than that of the control.

The decrease in efficiency in the PAP POSS cell could arise from various sources. Most likely, the PAP POSS is interfering with the efficiency of charge transport by

obstructing crystallite packing. Morphological studies provide further evidence of the action of the POSS molecules.

6.3 *Morphology changes*

Three different methods were used to probe morphology, each method providing information not available through the other two. The first method was X-ray Diffraction; this method produced information about the overall crystallinity, d-spacing between crystal layers and the crystallite domain size. The spectra obtained are found in Figure 6.3.1.

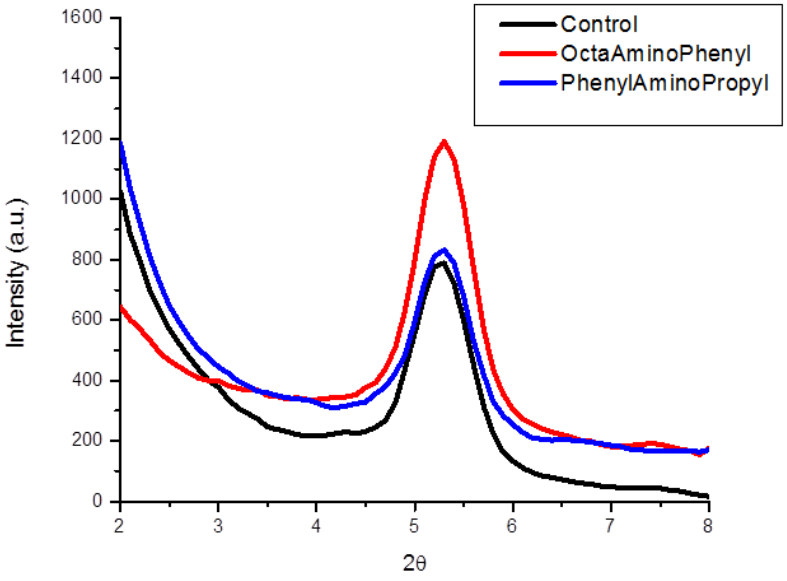

Figure 6.3.1. XRD Peaks for POSS Modified Active Layers.

The peaks in Figure 6.3.1 indicate that the addition of OAP POSS increases the crystallinity of the active layer over that of the control, which correlates with the

expected results. The area under the peak correlates with the overall crystallinity of the system; the integrated area for the A) Control was 95.76 B) OAP POSS was 97.39 and C) PAP POSS was 95.04. The data from the peaks were then used in conjunction with the Scherrer Equation to find the crystallite size in the samples.

The calculated relative crystallinity data obtained from Figure 6.3.1provide a contrast to the calculated sizes of the crystallite domains calculated using the Scherrer equation. The crystallite size can be seen in Figure 6.3.2. These crystallite sizes were calculated for each annealing state as well as each of the active layers.

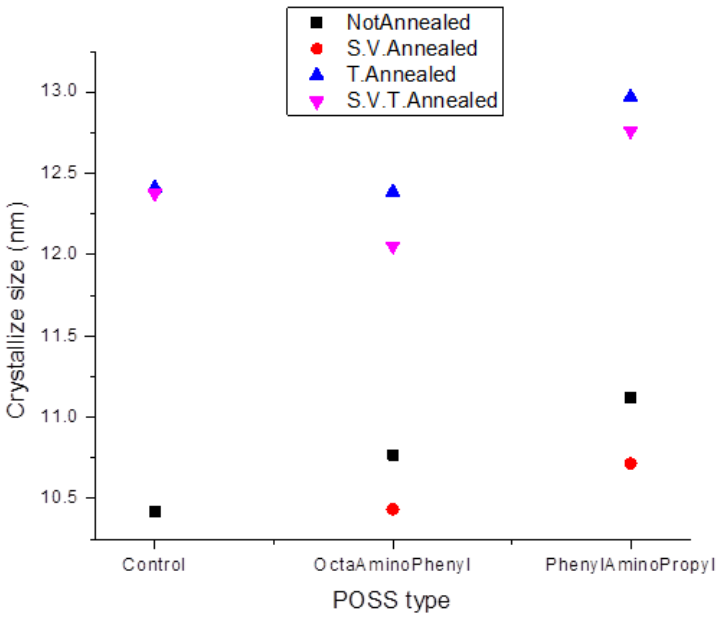

Figure 6.3.2. Crystallite Size of Neat and POSS-containing Samples at Various Annealing States.

This information indicates that the PAP POSS modified active layers had the largest crystallite domain size and OAP POSS modified active layer had the least. Large, coarse crystals often have pockets of amorphous content inside; this appears to be the

case with the PAP POSS. Amorphous areas would have shorter conjugation lengths, which would decrease the efficient transport of charge. It may also be that the crystallite is simply too large to diffuse across; an exciton needs an interface of about 10 nm or it decays. The crystallite domain size is also an indication of the crystallite domain width, and not the overall length of the crystallite. The overall result is that while the amount of crystallinity correlates with the efficiency trends within the samples measured, the crystallite size did not show a direct correlation with efficiency. The findings indicate that there is an optimal crystallite size. The crystallite size correlating with the most efficient cell (the solvent vapor and thermal annealed OAP POSS active layer) had a crystallite size of about 12 nm. The samples with smaller crystallites had significantly lower efficiencies, and those with larger crystallites showed decreases in efficiency with increase in size. Smaller crystallites might require the exciton to cross crystal grain boundaries, which have high resistance and would hinder transport. So somewhere between 11.2 nm and 12.0 nm there may be an optimal crystallite size that would correspond to an even greater efficiency than that demonstrated by the OAP POSS active layer.

The next method used to probe morphology was UV-Vis Spectroscopy. The spectra produced can be seen in Figure 6.3.3. This method provides information about the absorbance of the active layer as well as the relative crystallinity and degree of pi-pi stacking in the system. The importance of the absorbance of a cell is rather intuitive; if the cell does not absorb light, it cannot use the light to make excitons. Therefore, a sample that absorbs more light will most likely be more efficient.

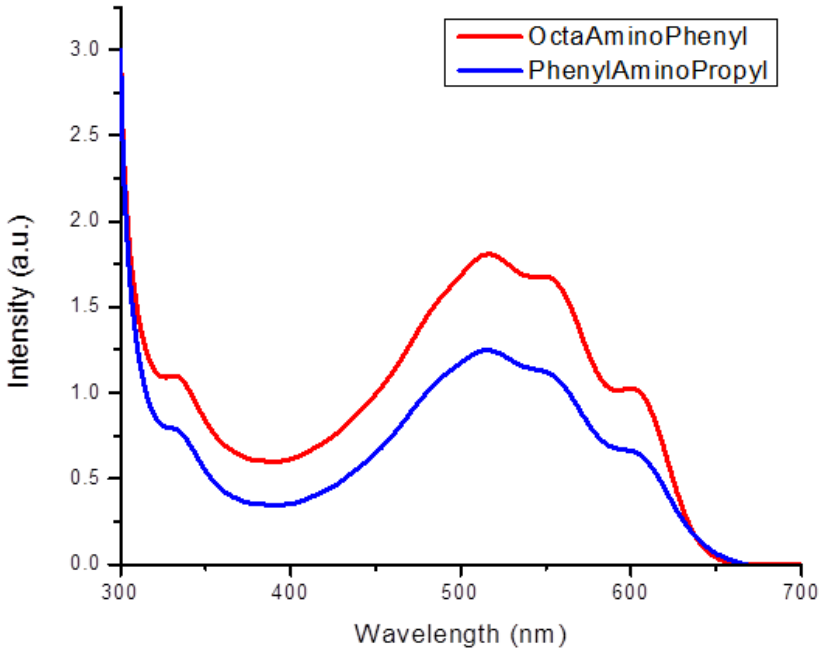

Figure 6.3.3. UV-Vis Spectra of POSS Modified Active Layers.

OAP POSS modified active layers absorb more light than their PAP POSS counterparts. The more pronounced shoulders on the OAP POSS curve, as seen in Figure 6.3.3, also indicate information about system. The shoulder at 325 nm indicates the higher crystallinity of the PCBM in the OAP system, while the shoulder near 600 nm indicates the greater extent of pi-pi stacking in the OAP POSS modified sample.[20] This is in agreement with our hypothesis that the POSS with the π electron cloud from the phenyl rings could facilitate inter-planar stacking of the donor polymer, thereby increasing the carrier mobility and device efficiency.

The third method used to investigate the morphology of the POSS-modified active layers was Atomic Force Microscopy. This method uses a tapping probe to produce an image of what the surface looks like on a nano-scale. This is the most visual

of the methods and the one that most easily demonstrates the radical changes in morphology that the POSS induces. Figure 6.3.4. is the height-image topography of the active layers. These AFM images show the distinct changes in morphology caused by the incorporation of POSS. Less distinct is the differences in average roughness; the control had an average roughness of 7.3 nm, PAP POSS 5.6 nm, and OAP POSS 4.1 nm.

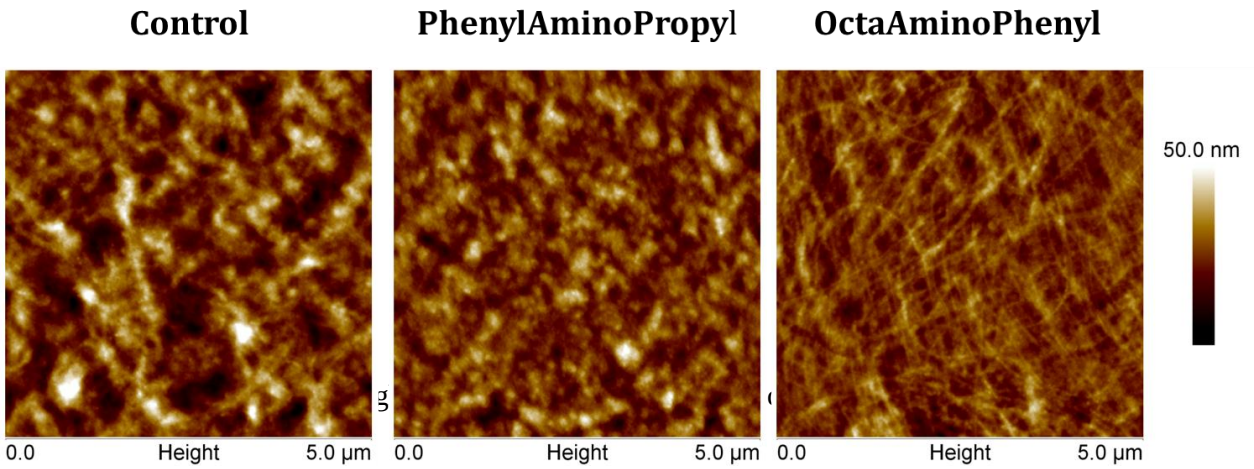

Both the control and the PAP POSS active layers displayed ellipsoidal oblong raised features of similar size, while the OAP POSS had a distinct change in morphology. It developed long, continuous fiber-like structure. These structures are about 3 µm long and extend across the length of the sample. This extended conjugation length increases the transport efficiency of the charges and is most likely what is causing the increase in the efficiency seen in the OAP POSS modified active layers.

CHAPTER VII

CONCLUSIONS

A standardized process was established that optimizes the annealing times and solvent used for annealing to have the maximum, reproducible efficiency in laboratory-scale OPV cells produced in air environment. This process used isopropanol in a twenty minute solvent vapor anneal and a thirty minute thermal anneal.

The addition of POSS to the active layer of an organic photovoltaic cell altered the morphology, and the change in morphology was dependent on the organic functionality of the POSS molecule. The modification by the planar, primary amine POSS (OAP) increased the efficiency by 20% over the control. It had a higher absorbance and greater crystallinity than both the control and the PAP POSS. Height AFM images displayed thin, continuous domains which are similar to the ideal morphology of separated domains that are continuous but have a large interface. The secondary amine with the non-planar phenyl ring POSS (PAP) containing active layer was less crystalline and absorbent, as well as less efficient. Its AFM images displayed similar ellipsoidal oblong features, a little bigger than those observed in the control.

There was also some evidence that there is an ideal crystallite domain size. PAP POSS had the largest domains, while OAP POSS had the least. However, unannealed and only solvent vapor annealing active layers had smaller crystallite sizes but were significantly less efficient. This seems to indicate that there is an ideal crystallite domain size, somewhere between 11 and 12 nm. Large crystallite domains do not correlate with higher crystallinity; these may have pockets that are amorphous. The crystallinity increases the conjugation length, which increases the charge mobility. If this is

interrupted, the efficiency of transport decreases and so does the overall efficiency of the cell. Also, if the crystallite is too small, the grain boundaries may be interrupting the charge. Crystal grain boundaries have a higher resistance than the rest of the crystal; it is possible that when more boundaries are encountered, as would happen with smaller crystallite sizes, the resistance would build to a greater extent and hinder transport. The data obtained in this study support our hypothesis that the primary amine with the planar phenyl ring (OAP)facilitates the formation of a more favorable morphology by the interaction of the π electron cloud with the conjugation of the D/A phase, causing greater packing and enhancing the overall efficiency.

RECOMMENDATION FOR FUTURE WORK

To gain a better understanding of the mechanisms of POSS interaction with the phase separated domains in the photoactive layer and the structural parameters that determine morphological changes, it is recommended that further characterization of the system be performed via conductive AFM, Raman spectroscopy and nuclear magnetic resonance spectroscopy. These findings should lead to recommendations for study of different POSS structures in other photoactive polymer blends to allow further increases in OPV power conversion efficiency.

REFERENCES

1. Green, M. A.; Emery, K.; Hishikawa, Y.; Warta, W. Solar Cell Efficiency Tables (Version 33). *Prog. Photovolt: Res. Appl.* **2009**, 17, 85-94.

2. Dennler, D.; Scharber, M. C.; Brabec, C.J. Polymer-Fullerene Bulk-Heterojunction Solar Cells. *Adv. Mater.***2009**, 21, 1323-1338.

3. Blom, P.W.M.; Mihailetchi, V.D.; Koster, L.J.A.; Markov, D.E. Device Physics of Polymer: Fullerene Bulk Heterojunction Solar Cells. *Adv. Mater.* **2007**, 19, 1551-1566.

4. Brabec, C.J.; Sariciftci, N.S.; Hummelen, J.C. Plastic Solar Cells. *Adv. Funct. Mater.* **2001**,11, 15-26.

5. Salamandra, L. Organic Photo-Voltaic Cells and Photo-Detector based on Polymer Bulk-Heterojunctions. Ph.D. Dissertaiton [Online], University of Rome, Rome, Italy, 2010. http://dspace.uniroma2.it/dspace/bitstream/2108/1294/1/PhD_Salamandra.pdf (accessed July 3, 2012).

6. Hoppe, H.; Sariciftci, N.S. Organic solar cells: An Overview. *J. Mater. Res.* **2004**, 19, 7, 1924-1945.

7. Nunzi, J-M. Organic photovoltaic materials and devices. *C.R. Phys* **2002**, 3, 523-542.

8. Bundgaard, E.; Krebs, F. C. Low bandgap polymers for organic photovoltaics. *Sol. Energy Mater. Sol. Cells.* **2007**, 91, 17, 954-985.

9. Nelson, J. Organic photovoltaic films. *Curr. Opin. Solid State Mater. Sci.* **2002**, 6, 87-95.

10. Ayzner, A. L.; Wanger, D.D.; Tassone, C. J.; Tolbert, S.H.; Schwartz, B.J. Room to Improve Conjugated Polymer-Based Solar Cells: Understanding How Thermal Annealing Affects the Fullerene Component of a Bulk Heterojunction Photovoltaic Device. *J. Phys. Chem. C.* **2008**, 112, 48, 18771-18716.

11. Clarke, T. M.; Ballantyne, A.M.; Nelson, J.; Bradley, D.D.C.; Durrant, J.R. Free Energy Control of Charge Photogeneration in Polythiophene/Fullerene Solar Cells: The Influence of Thermal Annealing on P3HT/PCBM Blends. *Adv. Func. Mater.* **2008**, 18, 24, 4029-4035.

12. Jo, J.; Kim, S-S.; Na, S-I.; Yu, B-K.; Kim, D-Y. Time-Dependent Morphology Evolution by Annealing Process on Polymer:Fullerne Blend Solar Cells. *Adv. Func. Mater.* **2009**, 19, 866-874.

13. Misra, R.; Fu, B.X.; Plagge, A.; Morgan, S. E. POSS-Nylon 6 Nanocomposites: Influence of POSS Structure on Surface and Bulk Properties. *J. Polym. Sci. B Polym. Phys.***2009,** 47, 1088–1102.

14. Paul, R.; Karabiyik, U.; Swift, M.C.; Esker, A.R. Phase Separation in Poly(tert-butyl acrylate)/Polyhedral Oligomeric Silsesquioxane (POSS) Thin Film Blends. *Langmuir*. **2008**, 24, 9, 5079-5090.

15. Li, C.; Chen, Y.; Wang, Y.; Iqbal, Z.; Chhowalla, M.; Mitra, S. A fullerene-single wall nanotube complex for polymer bulk heterojunction cells. *J. Mater. Chem.* **2007**, 17, 2406-2411.

16. Shrotriya, V.; Ouyang, J.; Tseng, R.J.; Li, G.; Yang, Y. Absorption spectra modification in poly(3-hexylthiophene):methanofullerene blend thin films. *Chem. Phys. Lett.* **2005**, 411, 138-143.

17. Guerrero, A., P. P. Boix, et al. "Oxygen doping-induced photogeneration loss in P3HT:PCBM solar cells." Solar Energy Materials and Solar Cells 100(0): 185-191.

18. Hu, Z., J. Zhang, et al. "Annealing-free, air-processed and high-efficiency polymer solar cells fabricated by a dip coating process." Organic Electronics 13(1): 142-146.

19. Wang, Y., L. Yang, et al. "Enhanced performance and stability in polymer photovoltaic cells using lithium benzoate as cathode interfacial layer." Solar Energy Materials and Solar Cells 95(4): 1243-1247.

20. Wu, S., J. Li, et al. "Investigation of high-performance air-processed poly (3-hexylthiophene)/methanofullerene bulk-heterojunction solar cells." The Journal of Physical Chemistry C 114(49): 21873-21877.